Electronic Supplementary Information

An organic transistor for the selective detection of tropane alkaloids utilizing a molecularly imprinted polymer

Qi Zhou,[a] Yui Sasaki,[a] Kohei Ohshiro,[a] Haonan Fan,[a] Valentina Montagna,[b] Carlo Gonzato,[b] Karsten Haupt*[b] and Tsuyoshi Minami*[a]

[a] Institute of Industrial Science, The University of Tokyo, 4-6-1 Komaba, Meguro-ku, Tokyo, 153-8505, Japan.
E-mail: tminami@iis.u-tokyo.ac.jp

[b] CNRS Enzyme and Cell Engineering Laboratory, Université de Technologie de Compiègne, Rue du Docteur Schweitzer, CS 60319, 60203 Compiègne Cedex, France
E-mail: karsten.haupt@utc.fr

CONTENTS

1. Characterization of the MIP and the extended-gate electrode

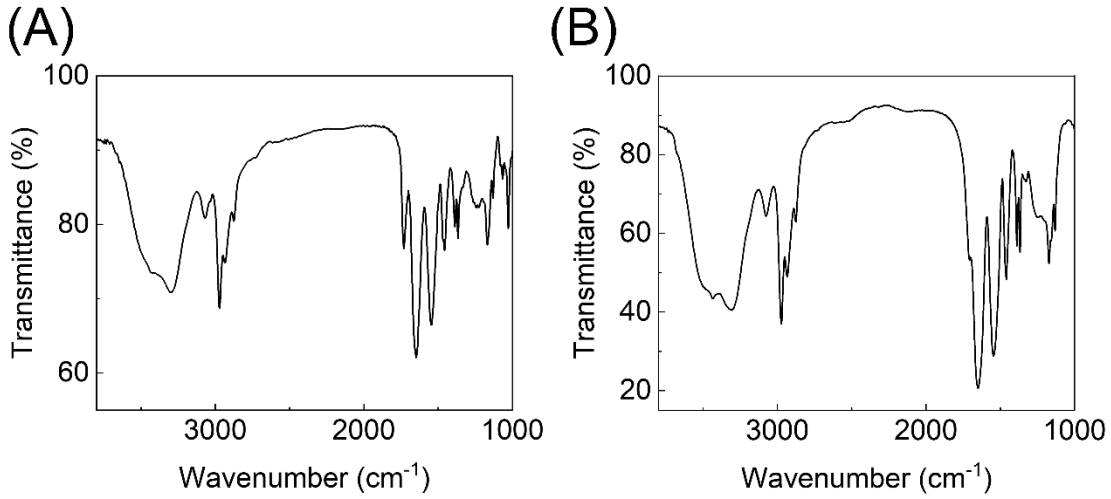

Fig. S1 FT-IR spectra (KBr pellet) of (A) imprinted *p*(NIPAM-*co*-DMPA-*co*-MBAAM) (MIP) and (B) non-imprinted *p*(NIPAM-*co*-DMPA-*co*-MBAAM) (NIP).

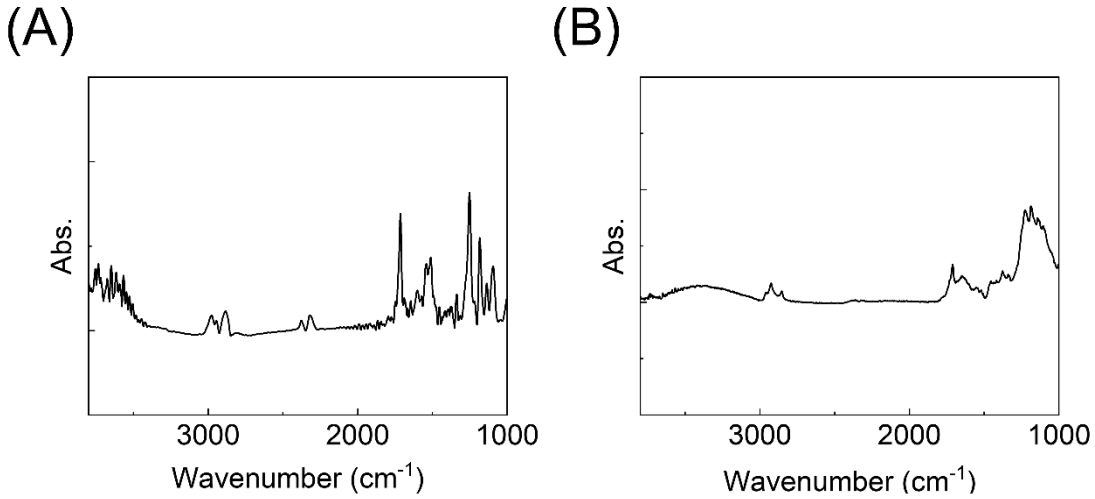

Fig. S2 FT-IR spectra (ATR) of (A) the MIP attached electrode and (B) the NIP attached electrode.

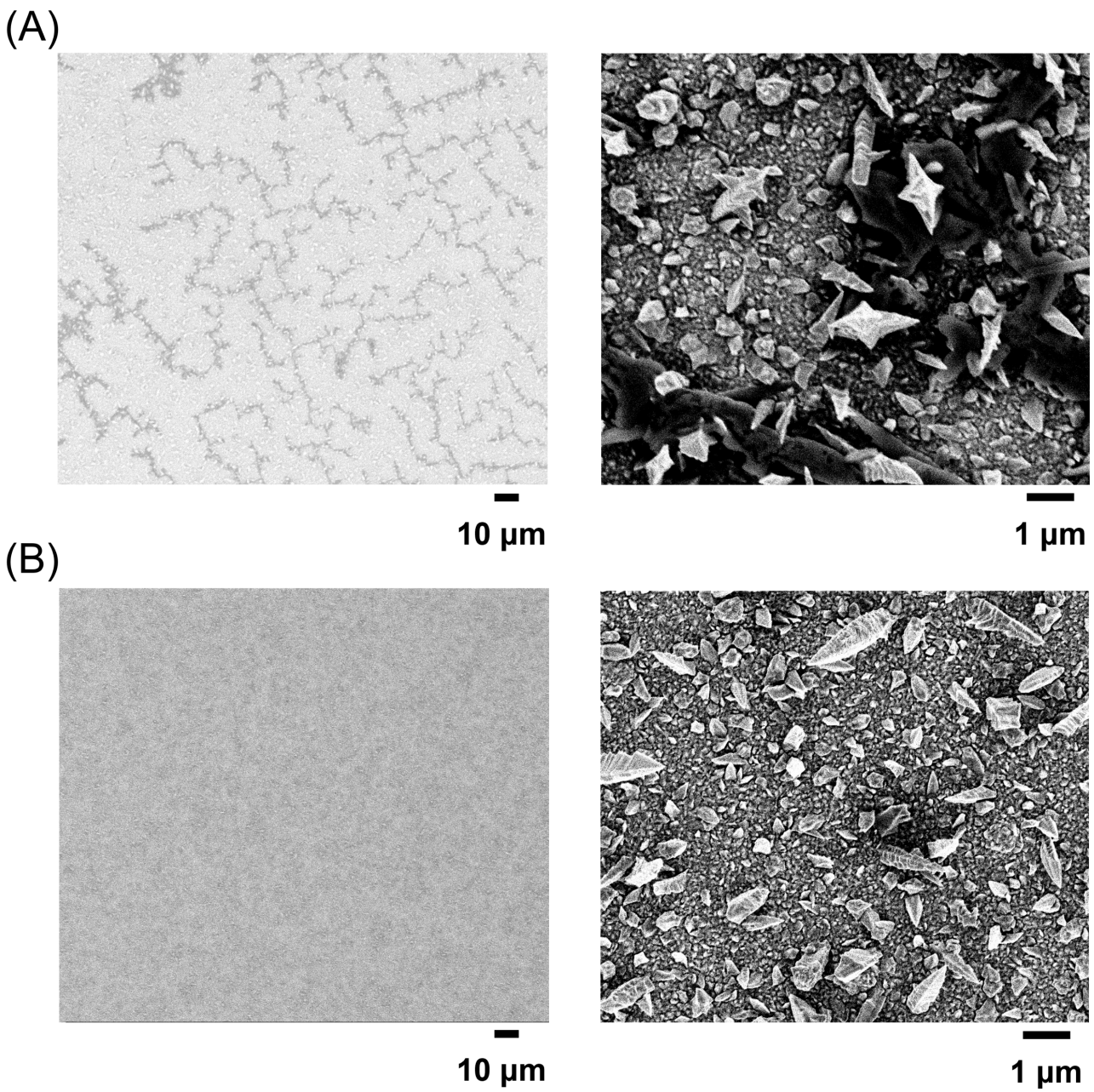

Fig. S3 FE-SEM images of (A) the MIP-AuNS electrode and (B) the NIP-AuNS electrode. The low magnified FE-SEM images indicated that the surface of the electrode was almost entirely covered with the polymer. In addition, sharp architectures derived from the AuNS layer could still be observed in the high magnified images.

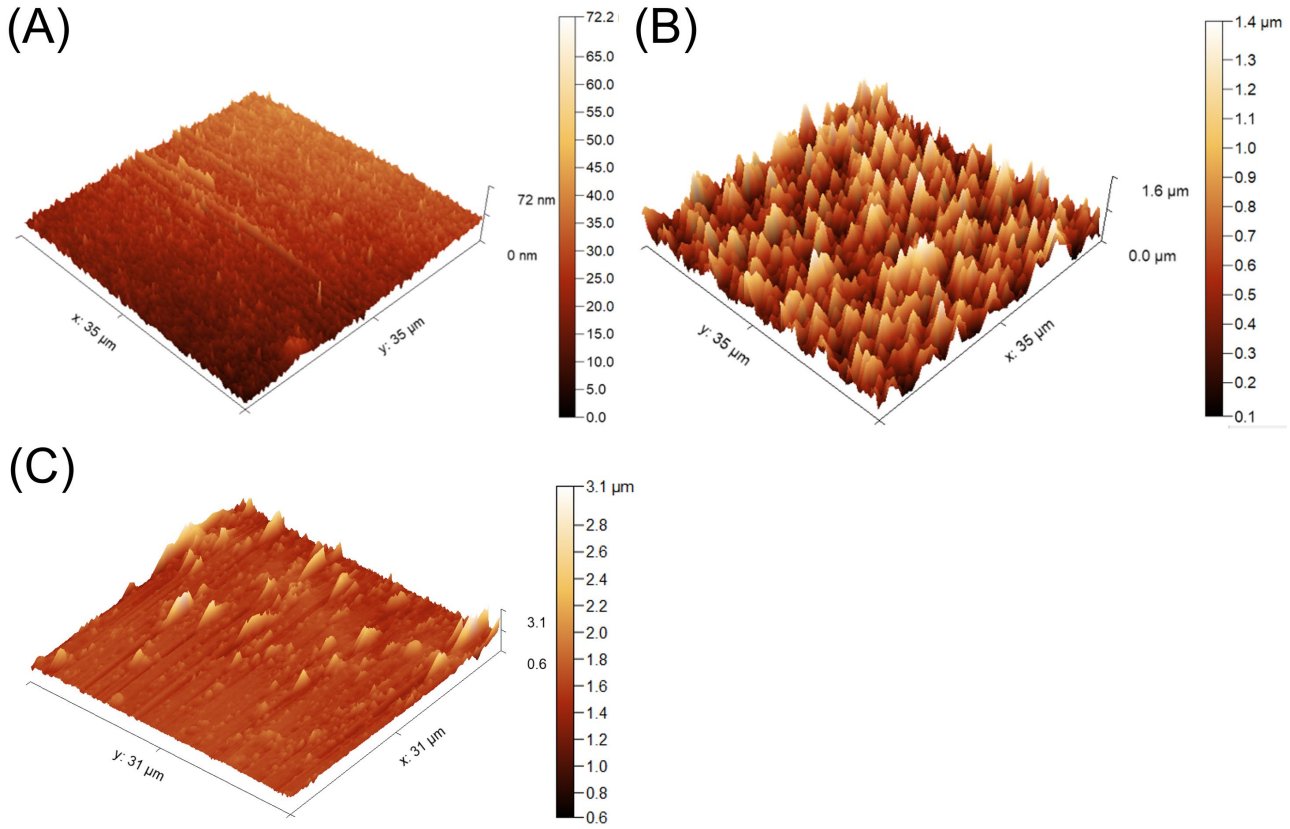

Fig. S4 FM-AFM Images of (A) the untreated extended-gate electrode, (B) the AuNS modified extended-gate electrode, and (C) the NIP attached AuNS modified extended-gate electrode.

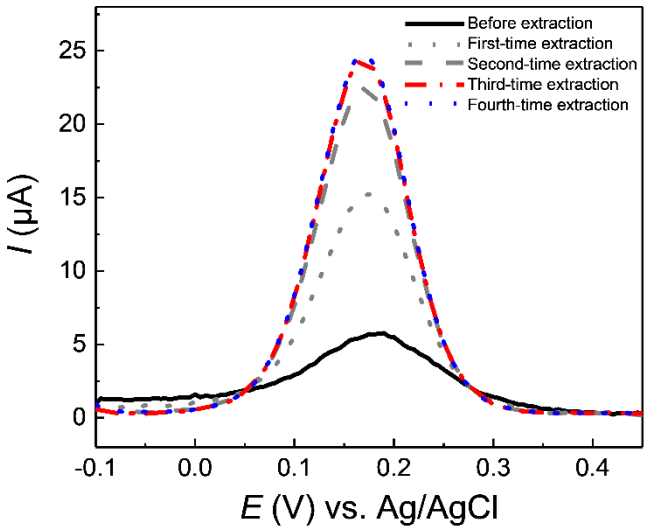

Fig. S5 DPV results of the MIP-AuNS electrode before (black solid line) and after first-time (gray dot line), second-time (gray dashed line), third-time (red dot and dashed line), and fourth-time (blue dot line) extraction in a phosphate buffer (100 mM, pH 7.0) containing $K_3Fe(CN)_6$ (5 mM) and KCl (100 mM) at 25 °C.

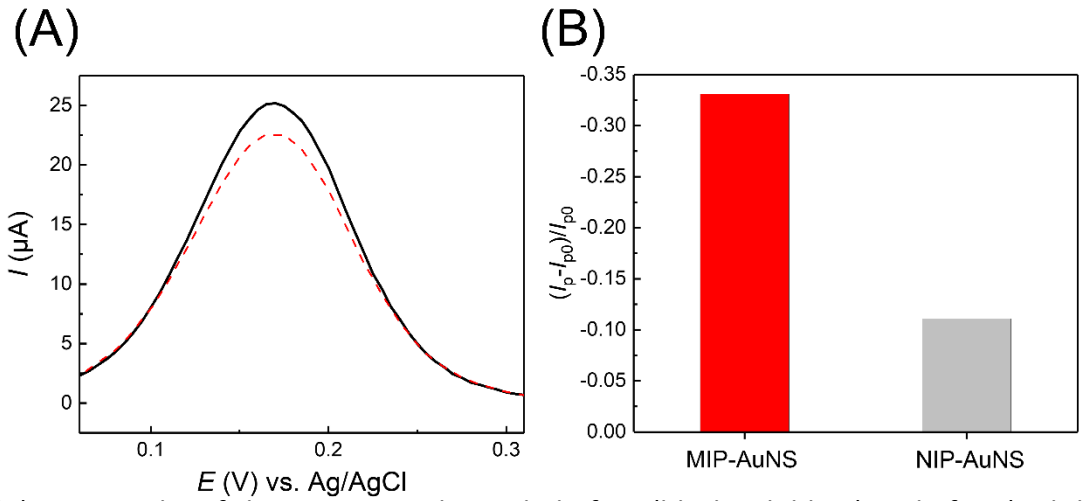

Fig. S6 (A) DPV results of the NIP-AuNS electrode before (black solid line) and after (red dash line) adding (*S*)-hyoscyamine (8.0 mM) in a phosphate buffer (100 mM, pH 7.0) containing $K_3Fe(CN)_6$ (5 mM) and KCl (100 mM) at 25 °C. (B) The comparison between the peak current (I_p) change of the MIP-AuNS electrode (red) and the NIP-AuNS electrode (gray) upon adding (*S*)-hyoscyamine (8.0 mM). The terms I_{p0} and I_P indicate the peak current before and after adding (*S*)-hyoscyamine, respectively.

Table S1 Comparison table of the binding energy

Ratio of NIPAM: DMPA:(*S*)-Hyoscyamine	Binding energy in water (kJ/mol)[a]	BSSE influence (kJ/mol)[a]	Corrected binding energy in water (kJ/mol)[a]
1: 1: 1	−87.29	2.22	−85.07
2: 1: 1	−98.56	2.46	−96.10
3: 1: 1	−102.24	2.76	−99.48
4: 1: 1	−110.82	3.08	−107.74

[a] The binding energies of the complexes at different molar ratios of NIPAM, DMPA, and (*S*)-hyoscyamine were evaluated by the DFT calculations. The complexes were optimized at B3LYP(D3BJ)/def2SVP level with IEFPCM solvent model (water) and were calculated at M06-2X(D3)/def2TZVP level with IEFPCM solvent model (water). The basis set superposition error (BSSE) influences were evaluated with the counterpoise method at M06-2X(D3)/def2TZVP level at vacuum conditions.

2. Fabrication and basic characteristics of the OFET

Fabrication scheme of the OFET

In addition to the procedure in the main manuscript, more detailed information is as follows. The glass substrate was washed with a piranha solution (H_2O_2:H_2SO_4 = 1:4, v/v) and Milli-Q water (18.2 MΩ cm) before the Al deposition. For fabricating an AlOx/TDPA dielectric layer, the aluminum oxide was immersed in a 2-propanol solution of tetradecylphosphonic acid (TDPA)[1] (10 mM) for 15 h at 25 °C. The concentration of PBTTT-C_{14} was 0.0125 wt%. The channel width and length were 50 μm and 1000 μm, respectively. For fabricating the semiconductive layer, the substrate was baked at 160 °C for 10 min. Finally, CYTOP™ (CTL-809M in CT-Solv.180, ratio 1 : 1, v/v) was coated on the organic semiconductor layer by a spin coater (MIKASA SPINCOATER 1H-D7), and the fully passivated OFET was baked at 110 °C for 10 min.

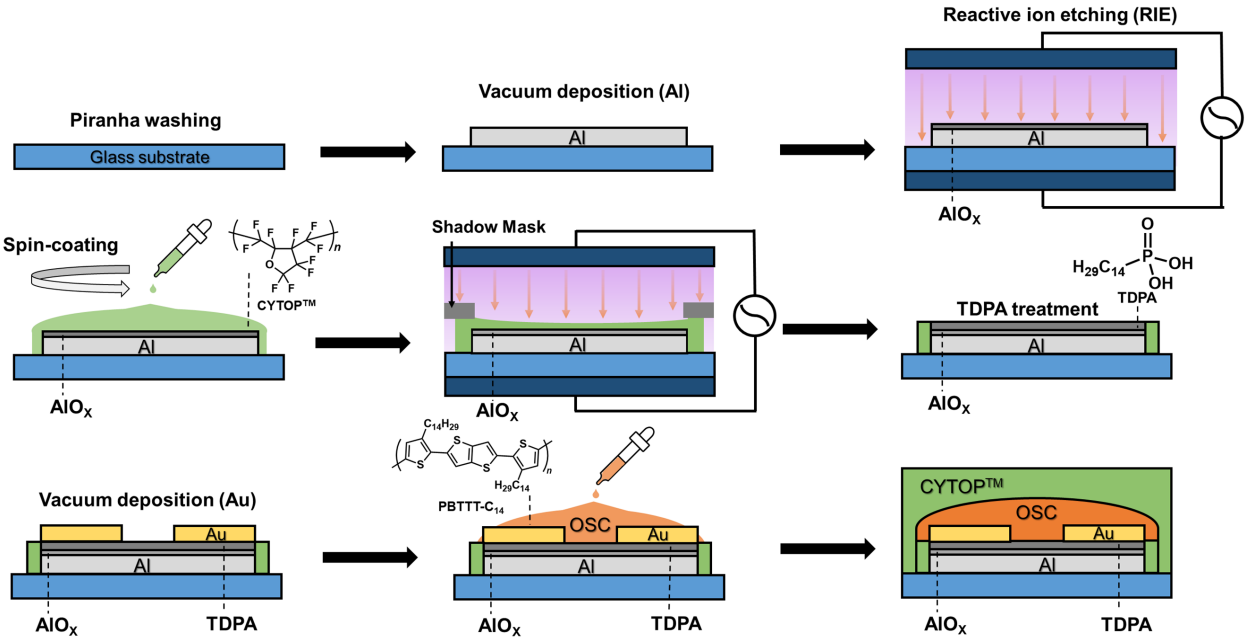

Scheme S1 Procedure for the OFET fabrication.

Basic characteristics of the OFET

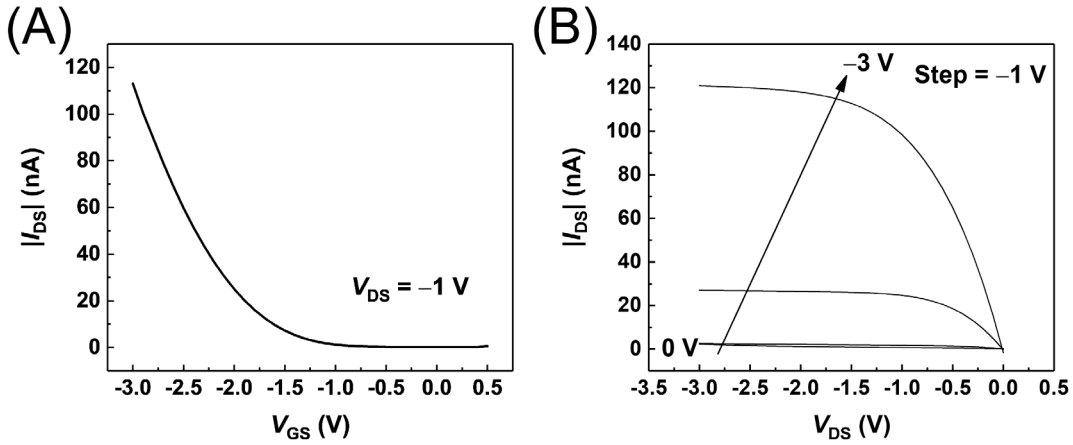

Fig. S7 (A) Transfer and (B) output characteristics of the fabricated OFET.

3. Selectivity test

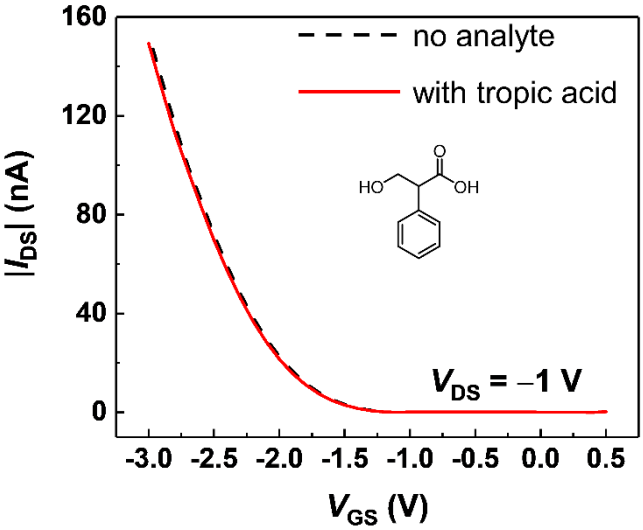

Fig. S8 Transfer characteristics of the MIP-OFET in a phosphate buffer (100 mM, pH 7.0) containing KCl (100 mM) at 25 °C (black dash line) and after adding tropic acid (5.0 μM) (red line).

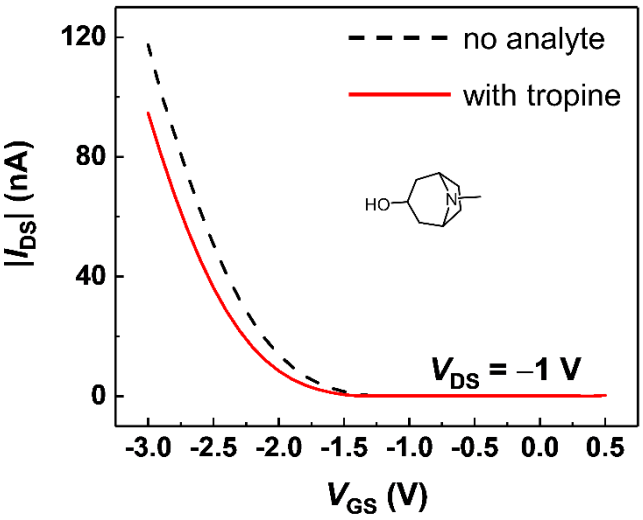

Fig. S9 Transfer characteristics of the MIP-OFET in a phosphate buffer (100 mM, pH 7.0) containing KCl (100 mM) at 25 °C (black dash line) and after adding tropine (5.0 μM) (red line).

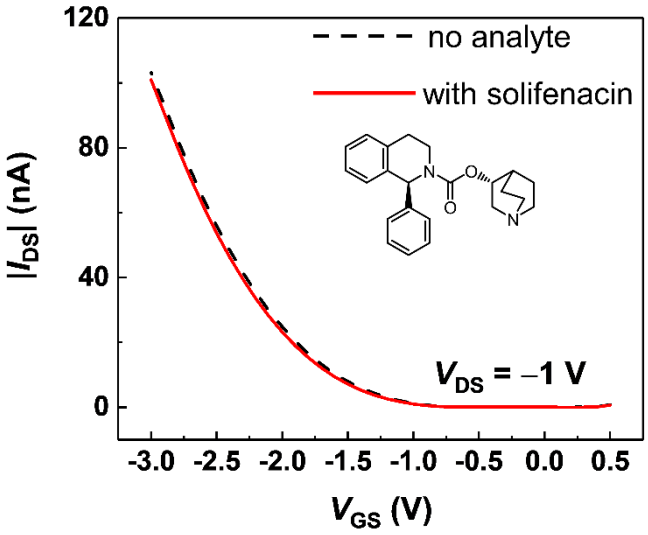

Fig. S10 Transfer characteristics of the MIP-OFET in a phosphate buffer (100 mM, pH 7.0) containing KCl (100 mM) at 25 °C (black dash line) and after adding solifenacin (5.0 μM) (red line).

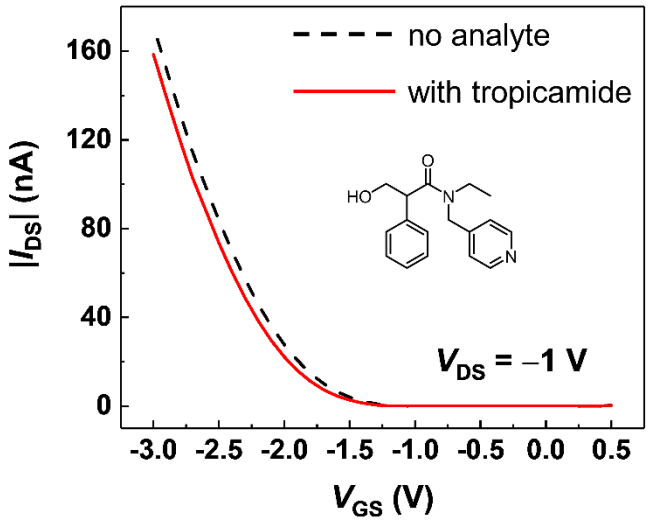

Fig. S11 Transfer characteristics of the MIP-OFET in a phosphate buffer (100 mM, pH 7.0) containing KCl (100 mM) at 25 °C (black dash line) and after adding tropicamide (5.0 μM) (red line).

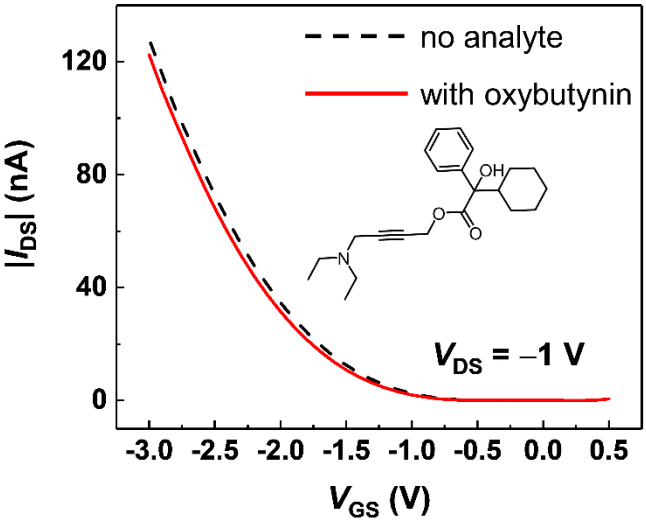

Fig. S12 Transfer characteristics of the MIP-OFET in a phosphate buffer (100 mM, pH 7.0) containing KCl (100 mM) at 25 °C and after adding oxybutynin (5.0 µM) (red line).

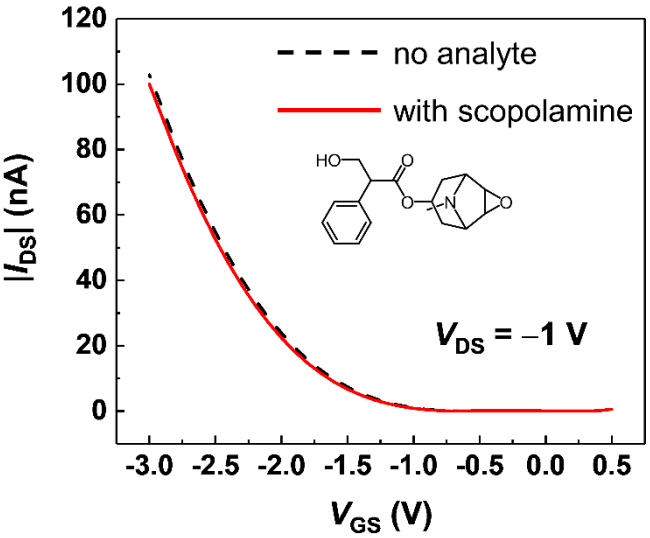

Fig. S13 Transfer characteristics of the MIP-OFET in a phosphate buffer (100 mM, pH 7.0) containing KCl (100 mM) at 25 °C and after adding scopolamine (5.0 µM) (red line).

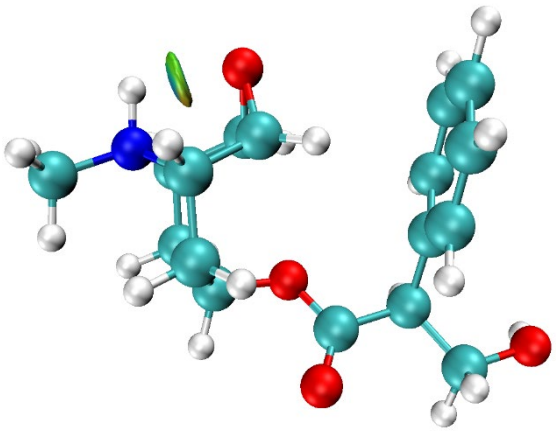

Fig. S14 The IGMH analysis result of the protonated scopolamine optimized by the DFT calculation. The isosurface between the oxygen atom of the epoxide moiety and the protonated tertiary amino group indicated the intramolecular hydrogen bond.

4. Determination of enantiomeric excess of (*S*)-hyoscyamine

Determination of enantiomeric purity of commercially available drugs by HPLC

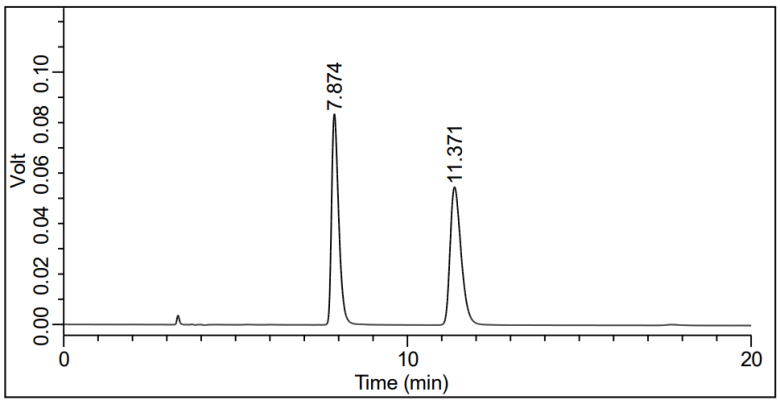

#	Time	Area	Area%	Height	Height%
1	7.874	1213063	49.90	83628	60.44
2	11.371	1217731	50.10	54748	39.56
		2430794	100.00	138376	100.00

Fig. S15 HPLC chart of the commercially available atropine by Daicel CHIRALCEL OZ-H. HPLC conditions were as follows: mobile phase: *n*-hexane:2-propanol:diethylamine = 80:20:0.1, v/v/v; flowrate: 1.0 mL/min; UV detector: 230 nm; column oven: 25 °C; injection volume: 10 µL.

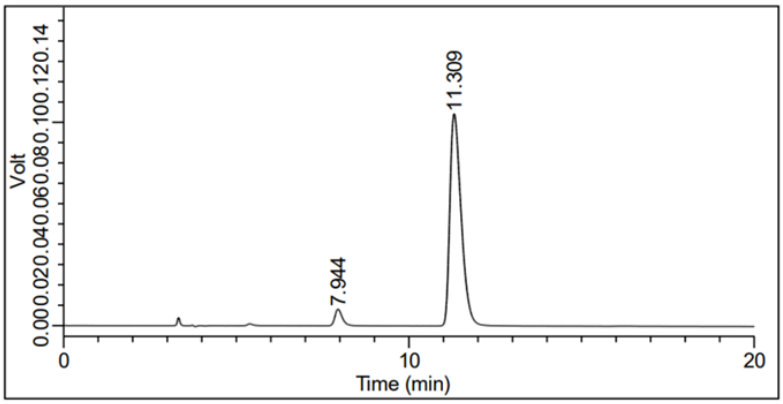

#	Time	Area	Area%	Height	Height%	Peak Name
1	7.944	122124	4.89	8192	7.27	
2	11.309	2377048	95.11	104427	92.73	(S)-Hyoscyamine
		2499172	100.00	112619	100.00	

Fig. S16 HPLC chart of the commercially available (*S*)-hyoscyamine by Daicel CHIRALCEL OZ-H. HPLC conditions were as follows: mobile phase: *n*-hexane:2-propanol:diethylamine = 80:20:0.1, v/v/v; flowrate: 1.0 mL/min; UV detector: 230 nm; column oven: 25 °C; injection volume: 10 µL.

Determination of % ee of (S)-hyoscyamine by the OFET

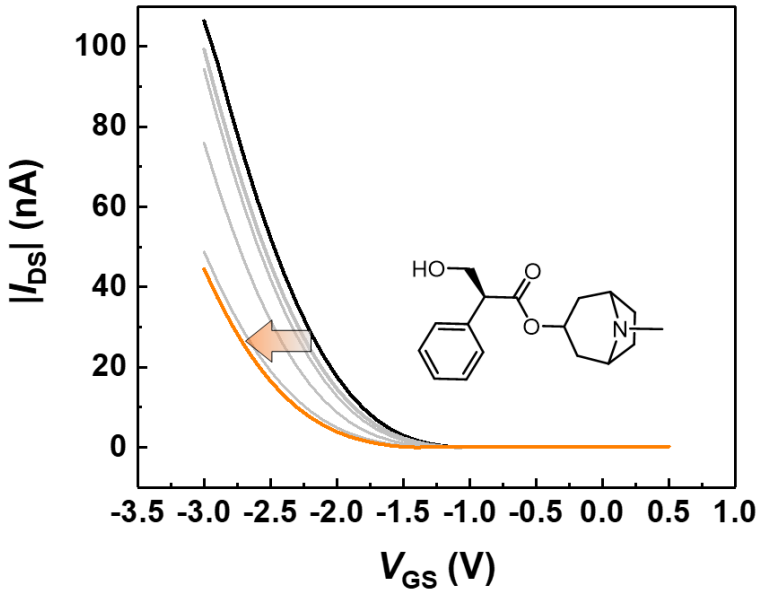

Fig. S17 Transfer characteristics of the MIP-OFET in a phosphate buffer (100 mM, pH 7.0) containing KCl (100 mM) at 25 °C (black solid line) and after adding hyoscyamine (5.0 µM) with different enantiomeric excesses of (*S*)-hyoscyamine (% ee values: 0.2, 22.7, 45.2, 67.7, 90.2).

Reference

1. M. Halik, H. Klauk, U. Zschieschang, G. Schmid, C. Dehm, M. Schütz, S. Maisch, F. Effenberger, M. Brunnbauer and F. Stellacci, *Nature*, 2004, **431**, 963-966.